JLAB USER GROUP

Jefferson Lab PAC15

Proposal Cover Sheet

This document must be received by close of business Thursday,

Dec 17, 1998 at:

Jefferson Lab
User Liaison,
Mail Stop 12B
12000 Jefferson Ave.
Newport News, VA
23606

Experimental Hall: A

Days Requested for Approval: 28

❒ Proposal Title:

Measurement of G_{E_p}/G_{M_p} to $Q^2 = 5.6$ GeV^2 by the recoil polarization method.

Proposal Physics Goals

Indicate any experiments that have physics goals similar to those in your propos

Approved, Conditionally Approved, and/or Deferred Experiment(s) or proposals:

None known to us.

Contact Person

Name: C. F. Perdrisat
Institution: College of William and Mary
Address: Physics Department, P.O. Box 8795
Address:
City, State, ZIP/Country: Williamsburg, VA 23187-8795 USA
Phone: (757) 221-3572 Fax: (757) 221-3540
E-Mail: perdrisat@cebaf.gov

Jefferson Lab Use On

Receipt, Date: 12/17/98 PR-99-007

By: [redacted]

HAZARD IDENTIFICATION CHECKLIST

JLab Proposal No.: _____ Date: December 17, 1998
(For CEBAF User Liaison Office use only.)

Check all items for which there is an anticipated need.

Cryogenics
- X beamline magnets
- X analysis magnets
- X target
  - type: _____
  - flow rate: _____
  - capacity: _____

Electrical Equipment
- _____ cryo/electrical devices
- _____ capacitor banks
- _____ high voltage
- _____ exposed equipment

Radioactive/Hazardous Materials
List any radioactive or hazadorous/ toxic materials planned for use:
_____
_____
_____
_____

Pressure Vessels
- _____ inside diameter
- _____ operating pressure
- _____ window material
- _____ window thickness

Flammable Gas or Liquids
- type: methane
- flow rate: _____
- capacity: _____

Drift Chambers
- type: VDC + straw tubes
- flow rate: _____
- capacity: _____

Other Target Materials
- ___ Beryllium (Be)
- ___ Lithium (Li)
- ___ Mercury (Hg)
- ___ Lead (Pb)
- ___ Tungsten (W)
- ___ Uranium (U)
- ___ Other (list below)

_____
_____

Vacuum Vessels
- _____ inside diameter
- _____ operating pressure
- _____ window material
- _____ window thickness

Radioactive Sources
- _____ permanent installation
- _____ temporary use
- type: _____
- strength: _____

Large Mech. Structure/System
- _____ lifting devices
- _____ motion controllers
- _____ scaffolding or
- _____ elevated platforms

Lasers
- type: None
- wattage: _____
- class: _____

Installation:
- _____ permanent
- _____ temporary

Use:
- _____ calibration
- _____ alignment

Hazardous Materials
- ____ cyanide plating materials
- ____ scintillation oil (from)
- ____ PCBs
- X methane
- ____ TMAE
- ____ TEA
- ____ photographic developers
- ____ other (list below)

_____
_____

General:

Experiment Class:
- X Base Equipment
- X Temp. Mod. to Base Equip.
- _____ Permanent Mod. to Base Equipment
- _____ Major New Apparatus

Other: _____
_____

BEAM REQUIREMENTS LIST

JLab Proposal No.: _____ Date: December 17, 1998

Hall: A Anticipated Run Date: 2000 PAC Approved Days: _____

Spokesperson: C.F. Perdrisat, M.K. Jones, V. Punjabi, E.T. Brash
Hall Liaison: _____
Phone: 221-3572
E-mail: perdrisat@cebaf.gov

List all combinations of anticipated targets and beam conditions required to execute the experiment. (This list will form the primary basis for the Radiation Safety Assesment Document (RSAD) calculations that must be performed for each experiment.)

Condition No.	Beam Energy (MeV)	Mean Beam Current (μA)	Polarization and Other Special Requirements (e.g., time structure)	Target Material (use multiple rows for complex targets — e.g., w/windows)	Material Thickness (mg/cm²)	Est. Beam-On Time for Cond. No. (hours)
1	4.845	105μA	0.40 (or 45μA,0.7)	Liquid Hydrogen	1g	36
2	4.845	same	same	"	"	84
3	5.545	same	same	"	"	192
4	6.045	same	same	"	"	360

The beam energies, E_{Beam}, available are: $E_{Beam} = N \times E_{Linac}$ where N = 1, 2, 3, 4, or 5. E_{Linac} = 800 MeV, i.e., available E_{Beam} are 800, 1600, 2400, 3200, and 4000 MeV. Other energies should be arranged with the Hall Leader before listing.

LAB RESOURCES LIST

JLab Proposal No.: _____ Date December 17, 1998

(For JLab ULO use only.)

List below significant resources — both equipment and human — that you are requesting from Jefferson Lab in support of mounting and executing the proposed experiment. Do not include items that will be routinely supplied to all running experiments such as the base equipment for the hall and technical support for routine operation, installation, and maintenance.

Major Installations *(either your equip. or new equip. requested from JLab)*

- exchange hadron and electron HRS detector packages
- install new FPP analyzer block
- weld one more electron support track

New Support Structures:

Data Acquisition/Reduction

Computing Resources: available

New Software: No

Major Equipment

Magnets: Standard

Power Supplies: Standard

Targets: Liquid Hydrogen 15 cm cell

Detectors: Standard

Electronics: Standard

Computer Hardware: Standard

Other:

Other:

PROPOSAL

Measurement of G_{Ep}/G_{Mp} to $Q^2 = 5.6$ GeV^2 by the recoil polarization method

Spokespersons

Charles F. Perdrisat and Mark Jones

College of William and Mary

Vina Punjabi

Norfolk State University

Edward J. Brash

University of Regina

ABSTRACT

The region of Q^2 from 1 to 10 GeV^2 has been anticipated to be where a transition from mesonic to quark-gluon degrees of freedom takes place. Measurements of the nucleon form factors in this region will directly test theories of the strong interaction. The magnetic form factor, G_{Mp}, of the proton is well known in this region, but the electric form factor, G_{Ep}, is poorly measured. E93-027 successfully ran during summer 1998 and measured G_{Ep}/G_{Mp} for Q^2 up to 3.5 GeV^2 using the recoil polarization technique. Previous measurements of G_{Ep} were inconsistent in this Q^2 range and the results from E93-027 clearly demonstrate that G_{Ep} and G_{Mp} have different Q^2 dependence. Given these results it is compelling to continue the mapping of the charge distribution by measuring G_{Ep}/G_{Mp} to larger Q^2. Only one experiment, which used the Rosenbluth separation technique, has measured G_{Ep} at Q^2 larger than 4.0 GeV^2.

Date : December 17, 1998

Lists of Participants

A. Deur
Jefferson Lab and Blaise Pascal University, Clermont-Ferrand, France

M. Epstein, D. Margaziotis
California State University at Los Angeles

C. Howell, S. Churchwell
Duke University/TUNL

B. Milbrath
Eastern Kentucky University

W. Boeglin, L. Kramer, P. Markowitz, B. Raue, J. Reinhold
Florida International University

R. Madey
Hampton University

L. Bimbot
Institut de Physique Nucléaire, Orsay, France

G. Quéméner
Institut des Sciences Nucléaires, Grenoble, France

E. Cisbani, S. Frullani, F. Garibaldi, M. Iodice and G.M. Urcioli
INFN-ISS, Italy.

P. Rutt
Jefferson Laboratory

N. Piskunov
LHE, JINR, Dubna, Russia

C. C. Chang
University of Maryland

W. Bertozzi, Z. Chai, K. Fissum, J. Gao, S. Gilad, N. Liyanage, M. Rvachev,
D. Rowntree, J. Zhao, Z. Zhou
Massachussetts Institute of Technology

J. Calarco
University of New Hampshire

M. Khandaker, V. Punjabi, C. Salgado
Norfolk State University

B. Vlahovic
North Carolina Central University

E. Brash, G. Huber, G. Lolos, Z. Papandreou, K. Benslama, J. Roche,
A. Fleck, N. Knecht, A. Shinozaki and C. Xuguang
University of Regina

S. Dieterich, R. Gilman, C. Glashausser, X. Jiang, G. Kumbartzki, S. Malov,
R. Ransome and S. Strauch
Rutgers State University

M. Jones, C.F. Perdrisat, O. Gayou, K. Wijesooriya
College of William and Mary

and the Hall A Collaboration

1 Introduction and Summary of Existing Data

In 1993 we proposed to measure the electric form factor (the Fourier transform of the charge distribution in the Breit frame) of the proton, G_{Ep}, to large four momentum transfer Q^2 with small error bars, by measuring the polarization of the recoiling proton in elastic $\vec{e}p \rightarrow e'\vec{p}$. We made the point at the time that the ratio of the transverse to longitudinal components of the transferred polarization was directly proportional to the ratio G_{Ep}/G_{Mp}, with the constant of proportionality being a factor depending on kinematical quantities only. The ratio is independent of both beam polarization and polarimeter analyzing power, because both polarization components are proportional to the product of these 2 quantities. Thus, unlike the traditional Rosenbluth separation, the polarization method gives directly the form factor ratio with one kinematical setup for each Q^2; the method is practically free of systematic uncertainties because only the beam helicity part of the polarization is required, and this is obtained by subtraction of data with positive and negative helicity, thus canceling all instrumental asymmetries.

PAC 6 approved the experiment, but only for 7 values of Q^2, up to a Q^2 of 3.5 GeV^2; our request was up to Q^2 of 4.5 GeV^2 with E_{beam} of 4 GeV and 6.0 GeV^2 with E_{beam} of 6 GeV. In May-June-July and August of 1998 in experiment 93-027 we measured G_{Ep}/G_{Mp} to Q^2 of 3.5 GeV^2 using the recoil polarization method. The absolute error bars on the new data range from 0.017 at Q^2=0.5 GeV^2 to 0.05 at Q^2=3.5 GeV^2 and are a distinct improvement on the previous measurements that used the Rosenbluth separation technique (especially for $Q^2 > 1.5$ GeV^2). The preliminary data are plotted in Fig. 1

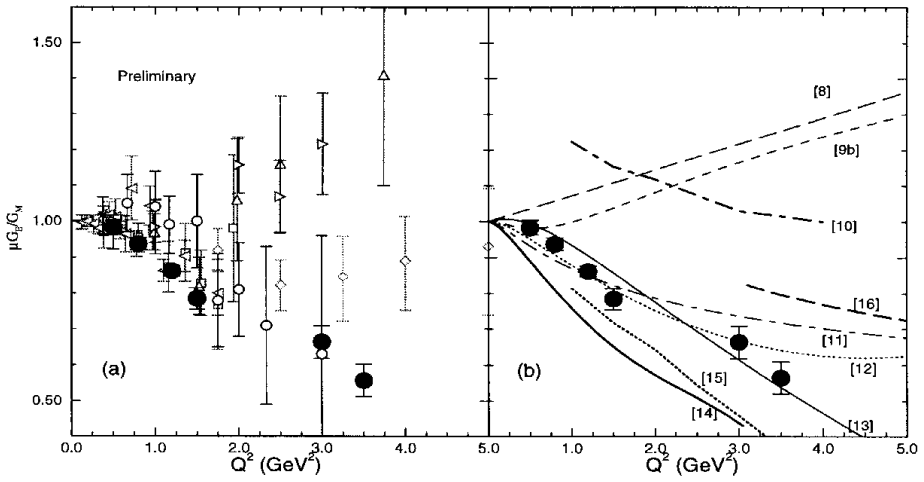

Figure 1: (a) Preliminary $\mu G_{Ep}/G_{Mp}$ from 93-027 (•) compared with previous world data (Ref [1]- [7]). (b) Theoretical predictions for same ratio (labels indicate reference number).

and one can clearly see a downward trend in the $\mu G_{Ep}/G_{Mp}$ ratio above Q^2=1 GeV^2, where earlier data had been more suggestive of a constant ratio. Four more data points, between Q^2 of 1.5 and 3.0 GeV^2, will become available soon. The striking feature of the new data is the fall-off of the $\mu G_{Ep}/G_{Mp}$ ratio from 1 starting at Q^2=0.5 GeV^2 to 0.55 at Q^2=3.5 GeV^2. This indicates that the shapes of G_{Ep} and G_{Mp} are different and the question immediately arises: will the drop-off in $\mu G_{Ep}/G_{Mp}$ continue, or slow down or will $\mu G_{Ep}/G_{Mp}$ rise back to 1? The answer to this question will have a significant impact on theories of the nucleons and models which use the nucleon form factors as inputs.

Already with the new data from Jefferson Lab, one can see that theories which predict $\mu G_{Ep}/G_{Mp}$ greater than one for $Q^2 > 1$ GeV^2 are eliminated. It can also be clearly seen that while Refs [12] and [13] are in approximate agreement up to $Q^2 = 3.5$, their behavior beyond this point is significantly different. A continuation to Q^2=5.6 GeV^2 with error bars comparable to what was achieved in 93-027 would clearly be of great interest by providing tighter constraints on models.

Given the results of 93-027 it is not difficult to see why most previous Rosenbluth separations did not give the correct $\mu G_{Ep}/G_{Mp}$ ratio: the rather rapid decrease of the ratio with increasing Q^2, compared to the dipole value, diminishes the contribution of G_{Ep} to the cross section correspondingly, making it even harder to measure than predicted on the basis of the dipole form factors, as illustrated in Fig. 2; here G_{Ep} has been extrapolated from a straight line fit to the 93027 data.

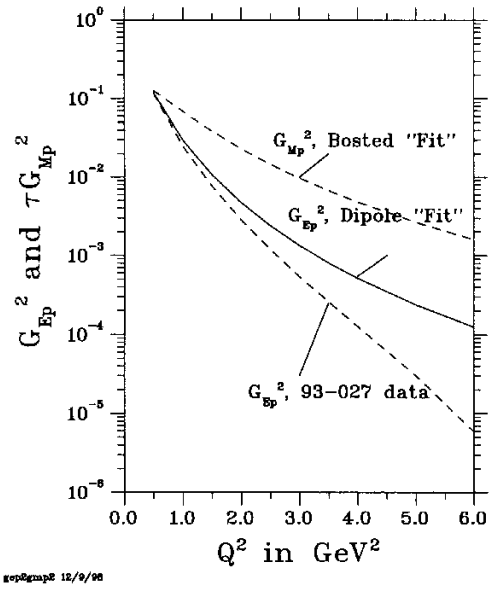

Figure 2: Contribution of the magnetic and electric form factors to the cross section; full line for dipole approximation and dotted line obtained by fitting the data

In Fig 3a the G_{Mp}/G_D ratio is plotted. G_{Mp} is with error bars smaller than 2% up to $Q^2 \approx 15$ GeV^2, and definitively starts to fall off below the dipole form factor around 6 GeV^2. In the Q^2 region where E93-027 measured G_{Ep}/G_{Mp}, G_{Mp} is measured to about 2% accuracy and has been parametrized by Bosted [19]. Using the Bosted parametrization, we can calculate G_{Ep}/G_D, and in Fig 3b G_{Ep}/G_D from Jefferson Lab is compared to previous data. In comparing G_{Ep}/G_D to G_{Mp}/G_D one should note the difference in the y-axis scale. G_{Mp}/G_D is 0.9 at $Q^2 \approx 10$ GeV^2 while G_{Ep}/G_D is already 0.55 at $Q^2 = 3.5$. This is a dramatic difference in the Q^2 dependence which contrasts with the expectation, before E93-027, that $\mu G_{Ep} = G_{Mp}$.

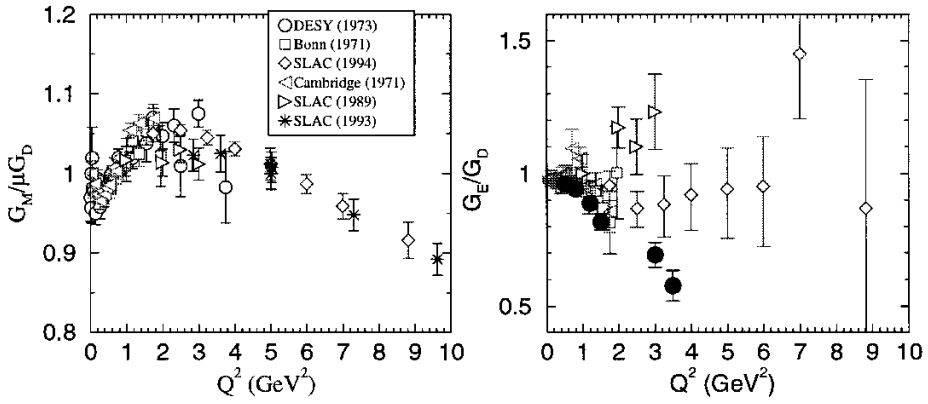

Figure 3: (a) World Data for $G_{Mp}/\mu G_D$. (b) Preliminary G_{Ep}/G_D from 93-027 (•) compared with previous world data

2 Theoretical Interest

The understanding of the structure of the nucleon has been of fundamental importance for the past several decades in nuclear and particle physics; ultimately such an understanding is necessary to describe the strong force. Certainly, for any QCD based theory, its ability to predict the pion and nucleon form factors correctly is perhaps the most important test of its validity, and hence precise data is required to test the models. The electromagnetic interaction provides a unique tool to investigate the structure of the nucleon.

The further characterization of G_{Ep} we are proposing here is one part of the JLab "Nucleon and Meson Form Factors and Sum Rules" program which includes precision measurements of G_{En} and G_{Mn}. The four elastic form factors of the nucleon are intimately connected, and this, perhaps, is most evident from recent vector meson dominance (VMD) calculations described below; obviously any QCD description of the nucleon will also have to be consistent with all four form factors.

The current operator can be expressed in terms of two form factors: F_1, the helicity conserving (Dirac) form factor, and F_2, the helicity non-conserving (Pauli) form factor. The Dirac and Pauli form factors can be related to the Sachs form factors G_E and G_M which, in the Breit frame, are the Fourier transforms of the charge and current distributions in the proton. The relationship between these two sets of form factors is $G_E = F_1 - \tau\kappa F_2$ and $G_M = F_1 + \kappa F_2$, where $\tau = Q^2/4M^2$ and κ is the anomalous magnetic moment of the proton.

At $Q^2 = 0$ one equates the form factors to their static values so that $G_M = \mu$ and $G_E = 1$. If one assumes an exponential shape for the charge and current distributions, the shape of the Sachs form factors is simply:

$$G_E = \frac{G_M}{\mu} = \left[\frac{m^2}{m^2 + Q^2}\right]^2$$

For $Q^2 < 1$ GeV^2 the experimental data can be reasonably described by such a form factor with $m^2 = 0.71$ GeV^2; this form is known in the literature as the dipole form factor, G_D. The same shape for the form factor also appears when one assumes that the interaction between the virtual photon and the nucleon is mediated by two vector mesons with similar masses and opposite phases; this is what is known as the Vector Meson Dominance model (VMD).

A better description of the data can be obtained by expanding the VMD to include exchanges of isovector and isoscalar mesons and their higher mass counterparts. Typically, the vector mesons are the ρ and its higher excited states for the isovector part, and the ω and ϕ for the isoscalar part of the nucleon form factor. The number of mesons involved in the interaction and the couplings and masses of the mesons can be varied to fit the data. But in practice the masses of the mesons are fixed to the free values and the number of mesons is limited to the minimum number necessary to give a reasonable fit to the data.

Given that VMD models are fits to the data, it may be more important to refit the models when new data become available, and see how that affects the parameters, than to make comparisons between the new data and old fits. In Fig. 1 the fits done in the 1970s in Ref. [12] and [13] come close to the 93-027 data, because the data available in the 1970s are compatible with the 93-027 data.

In the VMD model a constraint on the form factor at $Q^2 \to \infty$ is needed. Perturbative QCD has had success at high Q^2[20] and the calculation of Gari and Krumpelmann[9] incorporated such a pQCD constraint. The fit to the data existing in 1985 is shown in Fig. 4 as a solid line. When G_{Ep} was remeasured with smaller error bars in Ref. [6] for Q^2 between 1.0 and 3.0 GeV^2, a new fit was done by Gari and Krumpelmann which is shown in Fig. 4 as a dashed line. A large difference with the earlier fit is seen; the main difference in the calculations is a change in the form of the pQCD constraint required to fit the data [6]. The new data from Jefferson Lab clearly favor the older form of the pQCD constraint and it will be interesting to see what coupling constants, masses, and cut-offs emerge in a fit which includes the Jefferson Lab data.

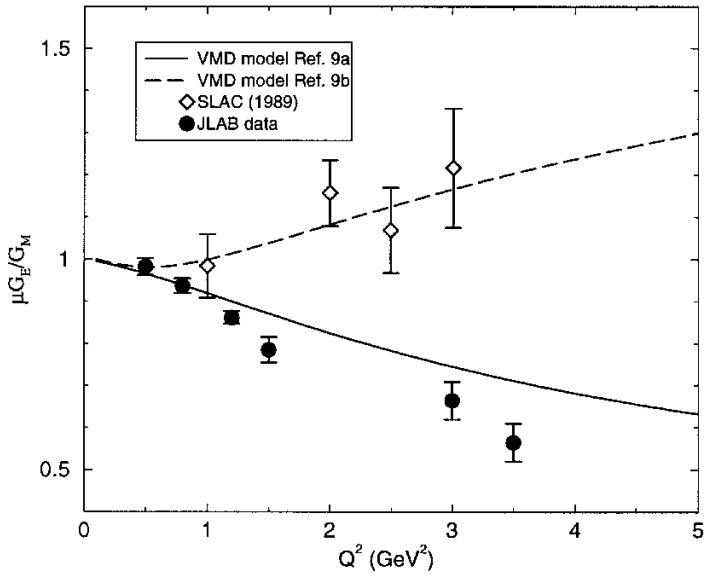

Figure 4: Comparison of two different parametrization of the VMD model of Gari and Krumpelmann to the Jefferson Lab data.

Mergell, Meissner and Drechsel[11] expanded on the the VMD model of Ref. [12] by incorporating the pQCD constraint at high Q^2 by a super-convergence condition. In this approach, the Dirac (F_1) and Pauli (F_2) form factors can be parametrized in a way which separates the hadronic (meson pole) and quark (pQCD) contributions to the form factor. The parametrization of the isoscalar part of the from factor is the following:

$$F^s_{1,2}(Q^2) = [\sum_s \frac{a^s_{1,2} L^{-1}(M_s^2)}{M_s^2 + Q^2}] L(Q^2) \tag{1}$$

where s represents the three isoscalar mesons masses in the fit and $a^s_{1,2}$ are the pole residues which can be related to the coupling constants. The isovector part of the form factors has a similar parametrization for the higher mass vector mesons, but the contribution from the ρ-meson is calculated from dispersion relations. $L(Q^2)$ has the following form:

$$L(M_s^2) = [\ln(\frac{\Lambda^2 + M_s^2}{Q_o^2})]^{-\gamma} \text{ and } L(Q^2) = [\ln(\frac{\Lambda^2 + Q^2}{Q_o^2})]^{-\gamma} \tag{2}$$

where $Q_o \approx \Lambda_{QCD}$ and γ is the anomalous dimension and is set to 2.148 . Λ^2 indicates the boundary where the quark contribution to the form factors becomes important.

In Fig. 5 the parametrization which was fitted to the form factor data (including Ref. [3] but not 93-027) is compared to the E93-027 data. Later the

database was expanded to include the form factors from the time-like region of Q^2 and the fit was redone and is plotted in Fig. 5 as a dashed line. The model is significantly closer to the E93-027 data. The main change in the model parameters is Λ^2 which changes from 9.73 GeV^2 in the fit to space-like data to 12.0 GeV^2 when the time-like data is included. To indicate the sensitivity of the model to the value of Λ^2 we have plotted in Fig. 5 the prediction we obtained with Λ^2 set to 14.0 GeV^2; it brings the model still closer to the data. This suggests that more precise data in the region above $Q^2 = 3.5$ GeV^2 will be critical in constraining Λ^2. The value of Λ^2 indicates the boundary between mesonic and quark degrees of freedom.

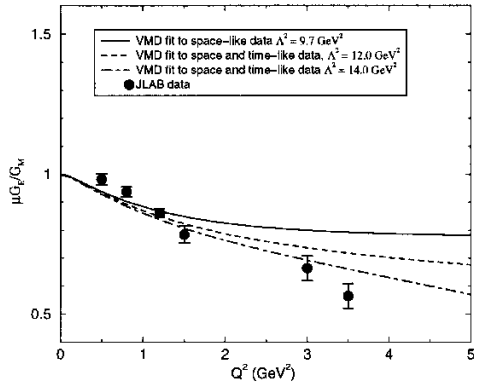

Figure 5: Comparison of three different parametrization of the VMD model of Hammer, Mergell, Meissner and Dreschel to the Jefferson Lab data demonstrating the sensitivity to the Λ^2 parameter which indicates the boundary between mesonic and quark degrees of freedom.

A number of theorists have extended the constituent quark model (CQM) in a relativistic way to medium Q^2 (1 to 6 GeV^2). Chung and Coester[8] investigated the dependence of the form factors on the constituent quark mass (m_q) and the range parameter defining the confinement scale ($1/\alpha$) in a relativistic CQM. In Fig. 1 their prediction is shown for a calculation using $m_q = .24$ GeV and $\alpha = .635$ GeV. At the time of their paper, these parameters gave reasonable agreement with the SLAC data of Ref.[6]. Ref.[8] indicates that G_{Ep} and G_{Mp} have a strong dependence upon the values of m_q and α at $Q^2 > 1.0$; new precision data may constrain m_q and α further. A more recent calculation of G_{Ep} and G_{Mp} in the light-front constituent quark model, by Frank, Jennings and Miller[15], indicates that G_{Ep} might change sign near 5.6 GeV^2; this calculation uses the light-front nucleonic wave function of Schlumpf[17].

Predictions of the nucleon form factors were done by Kroll, Schurmann and Schweiger [16] in a framework where the nucleon consists of quark and diquark constituents. In the limit of $Q^2 \to \infty$ the picture becomes the hard scattering formalism of pQCD. The parameters of the model were determined by fits to the ep cross sections above $Q^2 = 3.64$ GeV^2. Two sets of parameters gave equally

good fits to the *ep* cross sections, but differed markedly in their predictions for G_{Ep} and the neutron form factors. The diquark-quark model is not expected to be applicable below $Q^2 = 3$ GeV^2. A recent prediction[18] from this model is shown in fig. 1b, ref[16]. The range of validity of the di-quark model starts at 3 GeV^2, so increasing the Q^2 range will allow better testing of this model.

In Fig. 1 we also show the sum rule based prediction of Radyushkin[10]; the validity of this model is in the very large Q^2 region.

The version of the cloudy bag model used by Lu et al.[14] couples a pion field to the quarks inside a bag. As shown if Fig. 1 the prediction is low compared to the new Jefferson Lab data, but this is a simplified version of the model. Also, comparison to the ratio of the form factors is a more stringent test of a model. The authors suggest that one possible future development would be to include $\pi\pi$ interactions.

A comparison of the 93-027 data with model predictions is fraught with dangers at this time. Theoretical results have varied with experimental results, which, as we have shown above, have suffered from the limitations of the Rosenbluth separation in the past. Overall, VMD models are closest to the data, but they also have the strongest dependence upon the data input. It is thus probably fair to claim that the diversity of approaches and models examined so far gives a fair representation of the difficulties encountered in describing the internal structure of the nucleon; for an experimentalist this situation can only be interpreted as a strong motivation to continue the precision measurement of G_{Ep}.

3 The Recoil Polarization Method

In experiment 93-027 we used the recoil polarization method successfully to measure the ratio G_{Ep}/G_{Mp} up to Q^2 =3.5 GeV^2. Here we are proposing to use this same polarization technique to measure the G_{Ep}/G_{Mp}-ratio to Q^2 =5.6 GeV^2. The polarization method was first discussed by Akhiezer and Rekalo[21] and later by Arnold, Carlson and Gross [22]. With longitudinally polarized electrons one can either use a polarized target, or measure the transferred longitudinal and sideways polarizations, P_ℓ and P_t of the recoiling proton with a polarimeter. Starting above 1 GeV^2 this technique is superior to the traditional Rosenbluth separation technique: the main advantage of the polarization method, compared to the Rosenbluth method, is that it requires no change of energy or angle, for each Q^2 a single measurement of the azimuthal distribution of the protons diffused in a secondary scatterer determines simultaneously both P_ℓ and P_t.

As given in ref.[22], for one photon exchange, P_ℓ and P_t are:

$$I_0 P_l = \frac{1}{M}(E_e + E_{e'})\sqrt{\tau(1+\tau)}G_{Mp}^2 \tan^2\frac{\theta_e}{2} \quad (3)$$

$$I_0 P_t = -2\sqrt{\tau(1+\tau)} G_{Ep} G_{Mp} \tan\frac{\theta_e}{2} \quad (4)$$

where

$$I_0 = G_{Ep}^2(Q^2) + \tau G_{Mp}^2(Q^2)[1 + 2(1+\tau)\tan^2\frac{\theta_e}{2}] \quad (5)$$

The recoil polarization method was first used to obtain the neutron form factors in the $^2H(\vec{e}, e'\vec{n})$ reaction (Bates 88-05[23]). Bates experiment 88-21 also used the polarization transfer method to measure the form factor ratio G_{Ep}/G_{Mp} in $\vec{e}p \rightarrow e'\vec{p}$ at $Q^2 = 0.38$ and 0.50 GeV^2 for the free proton[7], as well as for the proton in the deuteron at recoil neutron momenta of 0 and 100 MeV/c[24] in $^2H(\vec{e}, e'\vec{p})n$, and the induced polarization in $^{12}C(\vec{e}, e'\vec{p})^{11}B$[25].

With a focal plane polarimeter, one measures the azimuthal angular distribution after a second scattering in an analyzer. This distribution has two components only, corresponding to the two projections of the polarization in the plane of the analyzer. It can be written as:

$$N_p(\theta, \varphi) = N_p(h=0)\epsilon(\theta)(1 \pm |h| A_c(\theta)[P_{t'} \sin\varphi - P_{n'} \cos\varphi]) \quad (6)$$

where |h| is the electron beam polarization, and the $\pm$ stands for the two possible orientations of the electron longitudinal polarization, N_p(h=0) is the number of protons incident on the polarimeter, θ, φ are the polar and azimuthal angles after scattering in the analyzer, $\epsilon(\theta)$ is the differential efficiency, and $A_c(\theta)$ the analyzing power of the analyzer, $P_{t'}$ and $P_{n'}$ are the in-plane components, transverse and normal, respectively, of the polarization at the analyzer.

For a spectrometer consisting of a single dipole with homogeneous field, the relation between polarizations at the analyzer and at the target can be written in terms of a spin transport matrix as:

$$\begin{pmatrix} P_{n'} \\ P_{t'} \\ P_{\ell'} \end{pmatrix}_{fp} = \begin{pmatrix} \cos\chi & 0 & \sin\chi \\ 0 & 1 & 0 \\ -\sin\chi & 0 & \cos\chi \end{pmatrix} \begin{pmatrix} P_n \\ P_t \\ P_\ell \end{pmatrix}_{tgt}$$

In the case of elastic ep scattering, P_n=0 in the single photon exchange approximation. Thus, in this case, in the single dipole approximation the relationship between target and focal plane components are:

$$P_{t'} = P_t \text{ and } P_{n'} = P_\ell \sin\chi \quad (7)$$

where χ is the spin precession angle in the spectrometer.

The Fourier analysis of the experimental azimuthal distribution $N_p(\theta, \varphi)$ in (4) gives the two physical amplitudes for each bin of θ:

$$a(\theta) = hA_c(\theta)P_t \text{ and } b(\theta) = hA_c(\theta)P_\ell \sin\chi \quad (8)$$

from which P_t and P_ℓ can be obtained.

The hadron HRS in Hall A consists of 3 quadrupoles and one dipole with shaped entrance and exit edges, as well as a radial field gradient. As a consequence further spin rotation occurs in these higher order magnetic fields (quadrupole, sextupole...). Therefore, the actual spin transfer matrix ($S_{n'm}$) has nine non-zero matrix elements. These matrix elements are different for every event, because they depend on $(\theta, y, \varphi, \delta)_{tgt}$. To extract the physical quantities P_t and P_ℓ one must correct for spin precession for each event. The method we have been using in the analysis is directly based on the Fourier analysis: one can show that the quantities a(θ) and b(θ) in Eq. 8 are the sums over all events in the azimuthal distribution, as follows:

$$a(\theta) = \frac{2}{N}[\sum_{i}^{N}(S^{(i)}_{n't}hA_c(\theta)P_t\cos^2\varphi_i + S^{(i)}_{n'\ell}hA_c(\theta)P_\ell cos^2\varphi_i)] \quad (9)$$

$$b(\theta) = \frac{2}{N}[\sum_{i}^{N}(S^{(i)}_{t't}hA_c(\theta)P_t sin^2\varphi_i + S^{(i)}_{t'\ell}hA_c(\theta)P_\ell \sin^2\varphi_i)] \quad (10)$$

where index i numbers the events. The equations can be solved for the 2 unknowns $(hA_c(\theta)P_t)$ and $(hA_c(\theta)P_\ell)$. The $S_{n'm}$ matrix elements have to be calculated from a model of the spectrometer. The spectrometer has been modeled with COSY, a differential analysis based code, and SNAKE, a ray-tracing code.

The ratio G_{Ep}/G_{Mp} can then be obtained directly from the ratio of $r(\theta)=\frac{hA_c(\theta)P_t}{hA_c(\theta)P_\ell}$:

$$G_{Ep}/G_{Mp} = -r(\theta)\frac{(E_e + E_{e'})}{2M}\tan(\frac{\theta_e}{2}) \quad (11)$$

The definition of P_t and P_ℓ (Eqns. 3 and 4) can then be used to calculate these two components from G_{Ep}/G_{Mp}, leading to a calculation of the quantity $hA_c(\theta)$. The beam polarization is measured independently with the Mott polarimeter at the injector, and with the Møller polarimeter in Hall A, thus providing a calibration of the polarimeter analyzing power for each of the proton energies of this proposal.

4 The polarimeter

The focal plane polarimeter (FPP) was built between 1993 and 1996 with instrumentation grants from NSF; it is mounted in the Hall A hadron spectrometer behind the VDC's. It consists of 4 tracking straw tube drift chambers, and a carbon analyzer. Each chamber is composed of 6 layers of straws. The first two chambers and the last chamber each have 3 V-layers and 3 U-layers, at $\pm 45^0$ relative to the dispersive direction (x). Chamber 3 has 2 U, 2 V and 2 X layers. In each set of U, V ,and X the individual planes are offset by half a straw from 1 plane to the next. The active areas of the first two chambers are 60x209 cm^2, chamber 3 124x272 cm^2 and chamber 4 142x295 cm^2. The total number of straws in the FPP is about 5200. In order to reduce the electronics

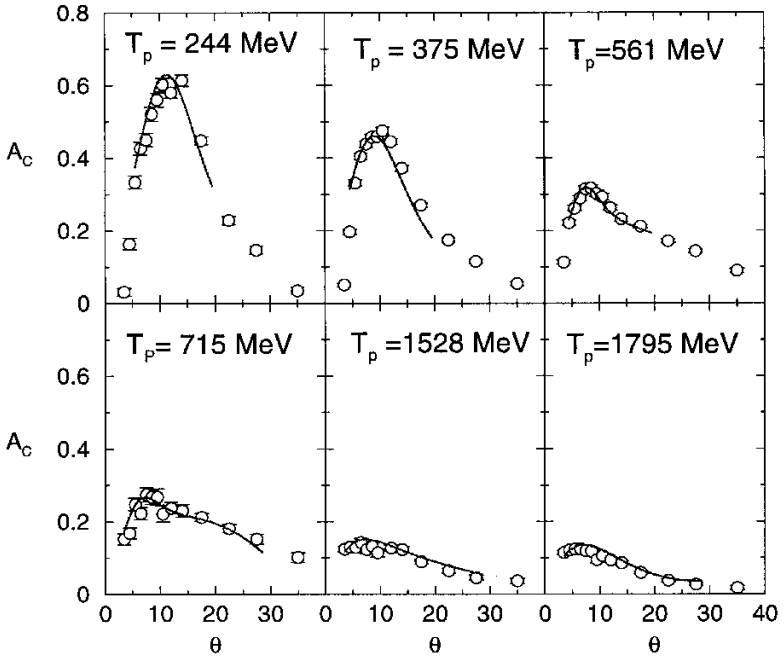

Figure 6: Analyzing powers of the Hall A focal plane polarimeter, as obtained in 93-027

required, sets of 8 straws are multiplexed. The effective spatial resolution of the straws is about 250 μm. The graphite analyzer in its present configuration consists of 5 sets of graphite plates, each with 2 plates left and right in each set. The thickness of the plates are 0.75, 1.5, 3.0, 6.0 and 9.0 inches. The density of the carbon is 1.70 gcm^{-3}.

The FPP was commissioned in the Spring of 1997, and was first used in experiment 89-033 with a proton energy of 400 MeV. Its efficiency was measured in the Spring of 1998 over the range of proton energies required for experiment 93-027 (0.586 to 1.6 GeV) for various thicknesses of graphite. The analyzing powers had been measured earlier in Los Alamos up to 800 MeV[26], and later in Saclay up to 2.4 GeV[27]. Experiment 93-027 also calibrated the polarimeter, as proposed in the original proposal. The analyzing power of the polarimeter was obtained as an independent result from the analysis of the azimuthal asymmetry distributions at each Q^2; it, of course, requires the independent measurement of the beam polarization which, during this experiment was measured using the Mott scattering polarimeter in the injection line of the accelerator, and with the recently commissioned Møller scattering polarimeter in Hall A. The calibration results from 93-027 for the analyzing power are compared in Fig. 6, with the Los Alamos fit up to 800 MeV, and the Saclay fit above this energy, over their respective angular ranges of validity.

Of great importance in spin transfer measurement is the understanding of spin precession in the HRS-H. Experiments 89-033 and 93-027 have given us a data base to investigate the contribution of the precession uncertainty to the total uncertainty. For example, data at Q^2=0.8 GeV^2 taken with 2 angles of the HRS-H, showed that, when using equations (7)-(9), the same G_{Ep}/G_{Mp}-ratio is obtained within the statistical uncertainty. Currently, we find that the dominant systematic uncertainty is on the vertical angle in the HRS-H, and it is about 2 mr (1σ); this will translate into systematic uncertainty of less than 0.01 for the points shown in fig. 1a.

Even though the simultaneous measurement of the sideways and longitudinal components of the proton polarization determines G_{Ep} independently of the analyzing power, A_c, and fraction of usable events in the analyzer, ϵ, the statistical uncertainty on G_{Ep} depends directly upon optimization of these two numbers. In fact it is the square of the coefficient of merit of the polarimeter, $\int_{\theta_{min}}^{\theta_{max}} A^2(\theta)\epsilon(\theta)d\theta$, which should be as large as possible. The only parameters available are the choice of the analyzer material and its thickness.

As expected, the results of 93-027 clearly indicate that the coefficient of merit becomes too small to continue this experiment to larger Q^2 with a carbon analyzer. Figure 7 shows the analyzing powers of pp scattering for 2.0, 3.0 and 4.0 GeV/c of Miller et al.[29].

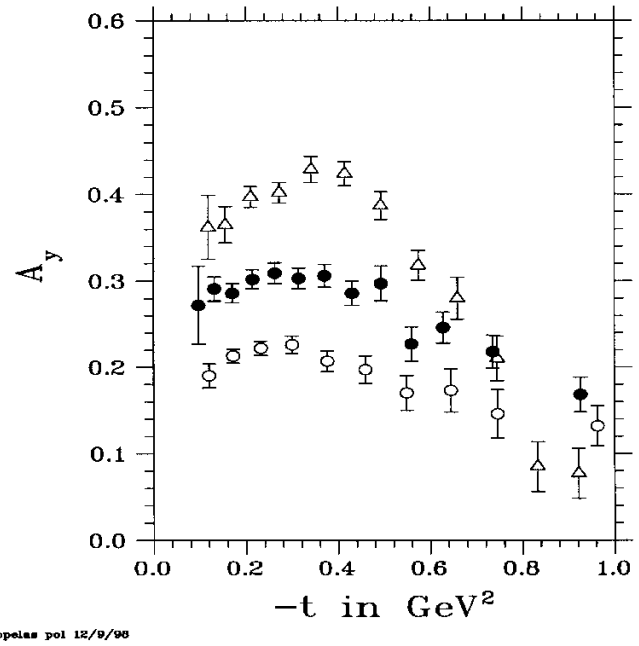

Figure 7: Analyzing power in pp, from ref.[29]: △ 2.0 GeV/c, • 3.0 GeV/c and ○ 4.0 GeV/c

At energies larger than 1 GeV, hydrogen is a much better polarization analyzer than carbon, as shown in Table 1.

Table 1: Analyzing power for hydrogen and carbon at different kinetic energies.

$T_p(GeV)$/p(GeV/c)→	1.05/1.75	1.27/2.0	1.73/2.5	2.20/3.0	3.17/4.0
Hydrogen[28]	0.4	0.38	0.32	0.25	0.2
Carbon[27]	0.2	0.17	0.14	0.11	0.07*

* indicates that the value is a guess based on extrapolation

A liquid hydrogen analyzer for the FPP is impossible because of the very large volume involved, perhaps 1-2 m^3. Several compounds contain partial hydrogen densities which are in fact larger than that of LH_2, 0.0798 gcm^{-3}. We considered several such compounds, and concluded that polyethylene $(CH_2)_2$ is good, and technically by far the simplest to handle.

In Table 2 the comparison of the coefficient of merit between carbon only, hydrogen only and polyethylene at the highest proton energy of 93-027, and at the

Table 2: The coefficient of merit (COM) and analyzing power (A_y) for different analyzer material at two kinetic energies. The COM have been corrected for small angles and neutrals.

material	COM	A_y	COM	A_y	ϵ
	T_p = 1.73 GeV		T_p = 3.00 GeV		
C	0.071	0.14	**0.036**	0.07	0.26
LH_2	0.078	0.32	0.049	0.20	0.06
$(CH_2)_2$	0.116	0.19	**0.075**	0.122	0.38

highest energy proposed here, demonstrates an improvement of $(0.075/0.036)^2$ = 4.3 over the time required for a given statistics, when replacing the present 50 cm of graphite with 70 cm of polyethylene. For $(CH_2)_2$, the coefficient of merit (COM) was calculated as $\sqrt{\epsilon_H A_H^2 + \epsilon_C A_C^2}$ and the analyzing power as $COM/\sqrt{\epsilon_H + \epsilon_C}$. The plan is to insert the $(CH_2)_2$ in the space created when the graphite blocks are in the open position.

5 Kinematics, Uncertainties and Rates estimates

To extend 93-027 beyond Q^2=3.5 GeV^2 will require a number of additional changes. The experiment would be best done with a beam polarization of approximately 0.70 with current of $45\mu A$; it requires energies up to 6 GeV. Comparable results, with 12% increase in error bars, would be obtained with smaller polarization and higher current (we have assumed 0.4 and 105 μA).

Table 3: Kinematics

E_e	Q^2	$E_{e'}$	θ_e	T_p	p	θ_p	χ	$d\sigma/d\Omega_e$	$A_y^2\epsilon$	rate
GeV	GeV^2	GeV	deg.	GeV	GeV/c	deg.	deg	cm^2/sr		Hz @105μA
4.845	3.5	2.980	28.5	1.865	2.642	32.6	241.	1.5×10^{-34}	0.0128	200
4.845	4.2	2.607	33.5	2.238	3.035	28.3	273.	4.4×10^{-35}	0.0097	67
5.545	4.9	2.934	31.9	2.611	3.423	26.9	305.	2.5×10^{-35}	0.0072	38
6.045	5.6	3.061	31.9	2.984	3.809	25.1	337.	1.3×10^{-35}	0.0057	20

Another change is required by the current limitation on the hadron HRS. Although the absolute Q^2 limit in Hall A defined by the maximum central momentum of the HRS's is 4 GeV/c, corresponding to a highest Q^2-value of 5.95 GeV^2, the current limitation on the hadron dipole (3.2 GeV/c) will require interchanging the detector packages between the electron and hadron HRS's. Preliminary discussions of the tasks involved indicate the swap could be done in one month. There is no intrinsic asymmetry between the two HRS's, except for the shower counters, but for this experiment the shower array is not necessary. The work to install the $(CH_2)_2$ blocks would be done as a natural part of the interchange, since the rear FPP chambers have to be removed for the exchange of the two detector packages, and also to insert the $(CH_2)_2$. The electron momentum remains smaller than 3.06 GeV/c for all kinematics planned (see Table 3).

We chose 5.6 GeV^2 as the maximum achievable value with the present instrumentation, including the interchange of the detector package. Relevant kinematical information, including cross sections in dipole approximation, can be found in Table 3, as well as the expected event rates in the focal plane, and the precession angle χ; also given in Table 3 are the square of the coefficient of merit. We are in the process of evaluating the radiative correction with the help of several theorists; the helicity dependence of the various radiative processes is commonly believed to be at the level of a few percents. Of course there is a trivial radiative corrections which affects the determination of Q^2 and can be calculated. A liquid hydrogen target with a useful length of 15 cm (1.0 gcm^{-2}) is assumed.

The anticipated results of the proposed experiment are shown in Fig. 8 and in Table 4. where the statistical uncertainties on a and b, the amplitudes from the Fourier analysis, are given by:

$$\Delta a(\theta) = \Delta b(\theta) = \sqrt{\frac{2}{\epsilon(\theta) N_p(\theta)}} \tag{12}$$

where $\epsilon(\theta)N_p(\theta)$ is the number of usable events within a given θ-bin. The χ-term in (10) is the systematic The uncertainties in Table 4 are calculated for h=0.4 and 0.7, with formula:

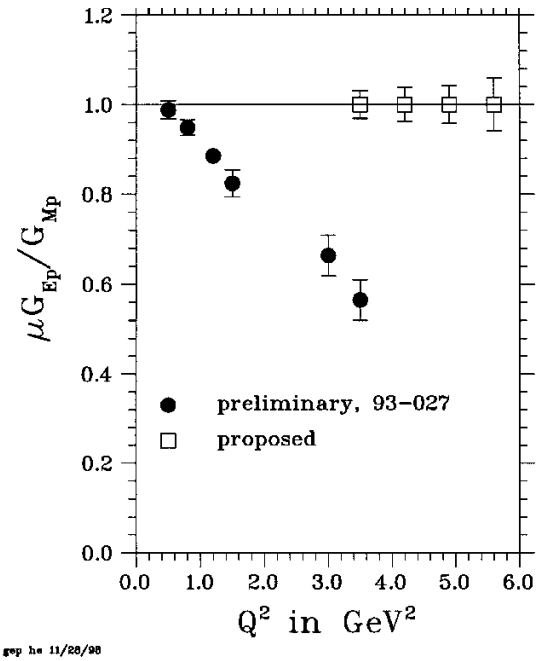

Figure 8: Illustration of the proposed data points, compared to PRELIMINARY results of 93-027

.

$$\frac{\Delta(G_{Ep}/G_{Mp})}{G_{Ep}/G_{Mp}} = \sqrt{(\Delta a/a)^2 + (\Delta b/b)^2 + (\Delta \sin\chi/\sin\chi)^2} \qquad (13)$$

uncertainty on the precession angle; based on our current understanding of the optics a value of 8 mr (1σ) has been assumed for all data points.

The relative uncertainty on G_{Ep}/G_{Ep} does directly depend on h and A_c through a and b in (10), but these need to be known only to the precision one requires on the uncertainty $\Delta(G_{Ep}/G_{Mp})$, rather than G_{Ep}/G_{Mp} itself. Additional sources of error from kinematical uncertainties on $\vec{q}_{e'}$ and $E_{e'}$, which determine Q^2, are very small.

There are intrinsic asymmetries in the polarimeter response; they may come from edge effects and anisotropies in the detection efficiency. The latter are eliminated by the usual cone test. In experiment 93-027 the fraction of events eliminated by the cone test was 4% at Q^2=3.5 GeV^2; it will keep decreasing as the proton energy increases toward Q^2=5.6 GeV^2. The residual instrumental asymmetry was found to be $\sim$ 0.005 averaged over the focal plane; the exact value depends sensitively upon the alignment of the FPP chambers. With the $(CH^2)_2$ in-place, straight through trajectories for alignment will be obtained from cosmics. In any event, the residual asymmetry is eliminated by switching of

Table 4: Proposed data points at which G_{Ep}/G_{Mp} will be measured, statistical uncertainties and times.

E_e	Q^2	absolute $\Delta(G_{Ep}/G_{Mp})$	time	absolute $\Delta(G_{Ep}/G_{Mp})$	time
GeV	GeV^2	h=0.4, I=105μA	hours	h=0.7, I=45μA	hours
4.845	3.5	0.035	36	0.031	36
4.845	4.2	0.043	84	0.038	84
5.545	4.9	0.048	192	0.042	192
6.045	5.6	0.066	360	0.059	360
		TOTAL TIME	672		672

the beam helicity for the helicity dependent part of the polarization components at the focal plane, and thus do not affect the ratio G_{Ep}/G_{Mp}. Furthermore, because the normal polarization component P_n is approximately 0 in elastic ep, the instrumental asymmetries can in fact be determined independently from the measured numbers of event $N_+(\theta,\varphi)$ and $N_-(\theta,\varphi)$, corresponding to the beam helicities h_+ and h_- , from the sum and difference spectra as follows:

$$N_+(\theta,\varphi) = N(h=0,\theta)\{1+(a+a_i)\sin\varphi-(b+b_i)\cos\varphi\}$$
$$N_-(\theta,\varphi) = N(h=0,\theta)\{1+(-a+a_i)\sin\varphi-(-b+b_i)\cos\varphi\}$$
$$N_+ - N_- -> a,b$$
$$N_+ + N_- -> a_i,b_i$$

where a_i and b_i are the instrumental asymmetries (and therefore independent of h).

From experiment 93-027 we know that the single's rates in electron and hadron arms are only a few times as large as the coincidence rate; therefore the accidental rate is negligible.

The total time requested according to the information in Table 4 is 672 hours with h=0.7 as well as with h=0.4; the total uncertainties will be typically 12% smaller with the larger beam helicity. In addition it will be necessary to obtain optics data with sieve slits at the highest Q^2. Sieve slit data for the electron HRS have been obtained in the VCS experiment up to 3.5 GeV/c; this will be the hadron detector in the proposed experiment, and therefore new sieve slit data are required only at 2.6 and 3.8 GeV/c. We anticipate the need for 4 days of Facility Development time for this task, preferably decoupled from the experiment proposed here.

6 Conclusion

Precision measurements of the four elastic form factors of the nucleon are required to test theories of the strong interaction. The Q^2 range accessible at

JLab is in the transition region from mesonic to quark-gluon degrees of freedom. G_{Mp} is known quite well in this region, but G_{Ep} was not until the results of JLab experiment 93-027; the neutron form factors will be measured in other experiments at JLab in the near future.

The data from experiment 93-027 have shown an unexpected and significant difference between the magnetic and electric form factors of the proton. Extending the Q^2 range beyond 3.5 GeV^2 will further map the electric form factor in this transition region.

We are proposing to continue the measurement of the ratio of the electric to magnetic form factors, G_{Ep}/G_{Mp},up to a $Q^2$of 5.6 GeV^2 using the recoil polarization method. In the Summer of 1998 Experiment 93-027 measured the same ratio up to Q^2=3.5 GeV^2, proving the viability of this method at large Q^2.

The advantage of this method over the Rosenbluth separation method, is that, for a given Q^2, it requires a polarization measurement at a single beam energy and electron scattering angle, whereas the separation technique typically requires 3 to 5 energies and angles. At Q^2=5.6 GeV^2 the error bars anticipated (systematics included) are 3-4 times smaller than obtained in the latest SLAC[3] experiment. In addition, the proposed experiment will calibrate the analyzing power of the polarimeter at 3 new proton energies.

References

[1] W. Bartel et al, Nuc. Phys. B58, (1973) 429.

[2] Ch. Berger, V. Burkert, G. Knop, B. Langenbeck, K. Rith, Phys. Letters 35B, (1971) 87.

[3] L. Andivahis et al, Phys. Rev. D 50, (1994) 5491. P. E. Bosted et al, Phys. Rev. Lett. 68, (1992) 3841.

[4] J. Litt et al, Phys. Letters 31B, (1970) 40.

[5] L. E. Price, J. R. Dunning, M. Goitein, K. Hanson, T. Kirk, and Richard Wilson, Phys. Rev. D 4, (1971) 45.

[6] R. C. Walker et al, Phys. Rev. D 49 , (1994) 5671. R. C. Walker et al , Phys. Lett. B 224, (1989) 353.

[7] B. Milbrath, J. McIntyre et al. , Phys. Rev. Lett 80 (1998) 452.

[8] P.L. Chung and F. Coester, Phys. Rev. D44, (1991) 229

[9] (a) M.F. Gari and W. Kruempelmann, Z. Phys. A322, (1985) 689. (b) M.F. Gari and W. Kruempelmann, Phys. Lett. B247 (1992) 159

[10] A.V. Radyushkin, Acta Phys. Polnica B 15, (1984) 40.

[11] P. Mergell, U.G. Meissner, D. Drechsler N.P. A596 (1996) 367 and A.W. Hammer, U.G. Meissner and D. Drechsel, P.L. B385 (1996) 343

[12] G. Hoehler et al. , Nucl. Phys. B 114, (1976) 505.

[13] F. Iachello, A.D. Jackson, A. Lande Phys. Lett. 43B (1973) 191.

[14] D.H. Lu, A.W. Thomas and A.G. Williams, Phys. Rev. 57 (1998) 2628

[15] M.R. Frank, B.K. Jennings and G.A. Miller, Phys. Rev. C54 (1996) 920

[16] P. Kroll, M. Schurmann and W. Schweiger, Z. Phys. A - Hadrons and Nuclei 338, (1991) 339.

[17] Felix Schlumpf, "Relativisitc Constituent Quark Model for Baryons", PhD thesis, University Zurich, (1992); see also SLAC-PUB-6502 (1994)

[18] P. Kroll, private communication (1998)

[19] P. E. Bosted, Phys. Rev. C 51, (1995) 409.

[20] S.J. Brodsky and G.P. Lepage, Phys. Rev. D22, (1981) 2157

[21] A. I. Akhiezer andd M. P. Rekalo, Sov. J. Particles Nucl. 3, (1974) 277.

[22] R. Arnold, C. Carlson and F. Gross, Phys. Rev. C23, (1981) 363.

[23] Eden et al., Phys. Rev. C 50 (1994) R1749.

[24] D. Barkhuff et al. submitted to Phys. Rev. Lett (1997).

[25] R. Woo et al. Phys.Rev. Lett 80 (1998) 456.

[26] M. W. McNaughton et al., NIM A241(1985) 435.

[27] E. Cheung et al., NIM A363 (1995) 561.

[28] Spinka et al. NIM 212 (1983) 239.

[29] D. Miller et al. Phys. Rev. D 16, 2016 (1977).